Mon. Not. R. Astron. Soc. **000**, 000–000 (0000) Printed 1 February 2008 (MN LATEX style file v1.4)

Millimetre/submillimetre-wave emission line searches for high-redshift galaxies

A. W. Blain,[1,2,3] D. T. Frayer,[2] J. J. Bock[4] and N. Z. Scoville[2]

[1] *Cavendish Laboratory, Madingley Road, Cambridge, CB3 0HE.*
[2] *Astronomy Department, California Institute of Technology, 105-24, Pasadena, CA 91125, USA.*
[3] *Institute of Astronomy, Madingley Road, Cambridge, CB3 0HA.*
[4] *Jet Propulsion Laboratory, 4800 Oak Grove Drive, Pasadena, CA 91109, USA.*

1 February 2008

ABSTRACT

The redshifted spectral line radiation emitted from both atomic fine-structure and molecular rotational transitions in the interstellar medium (ISM) of high-redshift galaxies can be detected in the centimetre, millimetre and submillimetre wavebands. Here we predict the counts of galaxies detectable in an array of molecular and atomic lines. This calculation requires a reasonable knowledge of both the surface density of these galaxies on the sky, and the physical conditions in their ISM. The surface density is constrained using the results of submillimetre-wave continuum surveys. Follow-up OVRO Millimeter Array observations of two of the galaxies detected in the dust continuum have provided direct measurements of CO rotational line emission at redshifts of 2.56 and 2.81. Based on these direct high-redshift observations and on models of the ISM that are constrained by observations of low-redshift ultraluminous infrared galaxies, we predict the surface density of line-emitting galaxies as a function of line flux density and observing frequency. We incorporate the sensitivities and mapping speeds of existing and future millimetre/submillimetre-wave telescopes and spectrographs, and so assess the prospects for blank-field surveys to detect this line emission from gas-rich high-redshift galaxies.

Key words: ISM: molecules – galaxies: evolution – galaxies: formation – cosmology: observations – infrared: galaxies – radio lines: galaxies

1 INTRODUCTION

The redshifted far-infrared/submillimetre-wave line emission from the interstellar medium (ISM) in galaxies could be exploited to detect new samples of distant gas-rich galaxies and active galactic nuclei (AGN) (Loeb 1993; Blain 1996; van der Werf & Israel 1996; Silk & Spaans 1997; Stark 1997; Combes, Maoli & Omont 1999; van der Werf 1999). This emission is attributable both to molecular rotational transitions, in particular from carbon monoxide (CO), and to atomic fine-structure transitions, in particular from the singly ionized 158-μm carbon [CII] line.

Redshifted CO emission has been detected from a range of known high-redshift galaxies and quasars in the millimetre/submillimetre waveband, as summarized by Frayer et al. (1998) and Combes et al. (1999). Many of these galaxies are known to be gravitationally lensed by a foreground galaxy, an effect which potentially complicates the interpretation of the results by altering the ratios of the inferred luminosities in the continuum and the detected lines (Eisenhardt et al. 1996). In only a small subsample of the detected galaxies (Solomon, Downes & Radford 1992; Barvainis et al. 1997; Downes et al. 1999) have multiple lines been detected, providing an opportunity to investigate the astrophysics of the ISM.

So far there have been very few detections of redshifted fine-structure lines, despite careful searches, for example, for both [CII] (Isaak et al. 1994; Ivison, Harrison & Coulson 1998a; van der Werf 1999) and singly ionized 205-μm [NII] emission (Ivison & Harrison 1996). Neutral carbon [CI] emission, which is considerably less intense than [CII] and [NII] emission in the Milky Way (Wright et al. 1991) and nearby galaxies (Stacey et al. 1991), has been detected from the gravitationally lensed Cloverleaf quasar (Barvainis et al. 1994). The most luminous high-redshift galaxies and quasars have necessarily been targetted in these searches.

[CII] fine-structure emission is powerful in both the Milky Way and in sub-L^* galaxies, in which it accounts for

about 0.5 per cent of the bolometric far-infrared luminosity (Nikola et al. 1998). However, based on observations of a limited number of low-redshift galaxies using the *Infrared Space Observatory (ISO)* (Malhotra et al. 1997; Luhman et al. 1998; Pierini et al. 1999), it appears that a systematically lesser fraction of the bolometric luminosity of more luminous galaxies appears as [CII] emission, about 0.1 per cent (Luhman et al. 1998). As noted by Luhman et al. (1998) and van der Werf (1999), the results of these *ISO* observations are fully consistent with the non-detection of redshifted fine-structure emission from high-redshift galaxies using ground-based submillimetre-wave telescopes. The results of Kuiper Airborne Observatory (KAO) observations of the Galactic centre (Erickson et al. 1991) indicate that 63- and 146-μm neutral oxygen [OI] fine-structure emission becomes steadily more luminous as compared with that from [CII] as the far-infrared luminosity of gas clouds increases. However, currently there is insufficient published data available to address this issue in external galaxies.

We attempt here to predict the counts of distant gas-rich line-emitting galaxies that could be detected in the millimetre/submillimetre waveband. There are two challenges to making reliable predictions. First, there are limited data available from which to construct a clear understanding of the astrophysics of the ISM in high-redshift galaxies. There are only a few tens of detections of line emission from these objects, the majority of which have been made in galaxies that are gravitationally lensed by foreground galaxies. Because of the potential for differential magnification across and within the lensed galaxy, neither the ratios of the line and continuum luminosities nor the excitation conditions in the ISM are known accurately in these cases. As shown by *ISO* [CII] observations, extrapolation of the observed properties of low-redshift galaxies with relatively low luminosities to greater luminosities in high-redshift galaxies is not necessarily reliable. Secondly, the space density and form of evolution of gas-rich galaxies at high redshifts has not been well determined. Thus the existing predictions of the observability of high-redshift submillimetre-wave line emission have concentrated on either discussing the potential observability of individual high-redshift galaxies (van der Werf & Israel 1996; Silk & Spaans 1997; Combes et al. 1999; van der Werf 1999), or have relied on extensive extrapolations, from the populations of low-redshift ultraluminous infrared galaxies (ULIRGs) (Blain 1996) and from low-redshift L^* bulges to the properties of proto-quasars at $z \sim 10$ (Loeb 1993).

Both of these difficulties can be addressed by exploiting the results of deep 450- and 850-μm dust continuum radiation surveys made using the Submillimetre Common-User Bolometer Array (SCUBA) camera (Holland et al. 1999) at the James Clerk Maxwell Telescope (JCMT; Smail, Ivison & Blain 1997; Barger et al. 1998; Hughes et al. 1998; Barger, Cowie & Sanders 1999; Blain et al. 1999b, 2000; Eales et al. 1999). These surveys are sensitive to galaxies at very high redshifts (Blain & Longair 1993), and have detected a considerable population of very luminous dust-enshrouded galaxies. The 15-arcsec angular resolution of the JCMT is rather coarse, but reliable identifications can be made by combining the SCUBA images with multi-waveband follow-up images and spectra (Ivison et al. 1998b, 2000; Smail et al. 1998, 2000; Barger et al. 1999b; Lilly et al. 1999), and crucially with observations of redshifted CO emission, which are currently available for two submillimetre-selected galaxies: SMM J02399−0136 at $z = 2.81$ and SMM J14011+0252 at $z = 2.56$ (Frayer et al. 1998, 1999; Ivison et al. 1998b, 2000). The bolometric and CO-line luminosities of these galaxies are reasonably well known, and because they are lensed by clusters rather than individual foreground galaxies, their inferred line ratios are not subject to modification by lensing. These observations thus provide a useful template with which to describe the properties of the ISM and line emission in high-redshift, dust-enshrouded, gas-rich galaxies.

In Section 2 we discuss the existing line observations, and summarize our current state of knowledge about the evolution and redshift distribution of galaxies that have been discovered in submillimetre-wave dust continuum surveys. In Section 3 we describe our model of line emission from these galaxies, and present the results, as based on our understanding of high-redshift continuum sources. In Section 4 we discuss the observability of this hypothetical population using existing and future millimetre/submillimetre-wave spectrographs. Unless otherwise stated, we assume that $H_0 = 50\,\mathrm{km\,s^{-1}\,Mpc^{-1}}$, $\Omega_0 = 1$ and $\Omega_\Lambda = 0$.

2 BACKGROUND INFORMATION

2.1 Line observations

Ground-based telescopes have detected molecular rotation lines and atomic fine-structure lines from low-redshift galaxies (e.g., Sanders et al. 1986; Wild et al. 1992; Devereux et al. 1994; Gerin & Phillips 1999; Mauersberger et al. 1999). Atomic fine-structure lines have also been observed from bright galactic star-forming regions and nearby galaxies using the KAO (Stacey et al. 1991; Nikola et al. 1998), *COBE* (Wright et al. 1991) and *ISO* (Malhotra et al. 1997; Luhman et al. 1998; Pierini et al. 1999).

CO rotational line emission has been detected successfully from various high-redshift galaxies and quasars, including the first identified high-redshift ULIRG *IRAS* F10214+4724 (Solomon et al. 1992), the gravitationally lensed Cloverleaf quasar H 1413+117 (Barvainis et al. 1994; Kneib et al. 1998), various quasars at $z \simeq 4$, including BR 1202−0725 (Ohta et al. 1996, 1998; Omont et al. 1996) and the extremely luminous APM 08279+5255 (Lewis et al. 1998; Downes et al. 1999), and the submillimetre-selected galaxies SMM J02399−0136 and SMM J14011+0252 (Frayer et al. 1998, 1999). A significant fraction of the dynamical mass in many of these systems is inferred to be in the form of molecular gas, and it is plausible that they are observed in the process of forming the bulk of their stellar populations.

2.2 Atomic fine-structure lines

Atomic fine-structure lines emitted at wavelengths longer than about 100 μm – [CII] at 1900 GHz, [NII] at 1460 and 2460 GHz, [OI] at 2060 GHz, and [CI] at 492 and 809 GHz – are redshifted into atmospheric windows for galaxies at redshifts $z \lesssim 5$, the redshift range within which at least 80 per cent of dust-enshrouded galaxies detected by SCUBA appear to lie (Smail et al. 1998; Barger et al. 1999b; Lilly et al. 1999). There are many other mid-infrared lines with

shorter restframe emission wavelengths (see, e.g., Lutz et al. 1998); however, unless massive galaxies exist at $z \sim 10$, these lines will not be redshifted into atmospheric windows accessible to ground-based telescopes.

Here we assume that the line-to-bolometric luminosity ratio $f_{\rm line} = 10^{-4}$ for the [CII] line in all high-redshift gas-rich galaxies, corresponding to the value observed in low-redshift ULIRGs. The equivalent value for $[{\rm CI}]_{492\,{\rm GHz}}$, $f_{\rm line} = 2.9 \times 10^{-6}$ is chosen to match the value observed by Gerin & Phillips (1999) in Arp 220. The values of $f_{\rm line}$ for other fine-structure lines listed in Table 1 are chosen by scaling the results of observations of the Milky Way and low-redshift galaxies (Genzel et al. 1990; Erickson et al. 1991; Stacey et al. 1991; Wright et al. 1991). This approach should lead to a reliable estimate of the counts of [CI] and [CII] lines, but greater uncertainty in the N and O line predictions. In the absence of more observational data, which would ideally allow luminosity functions to be derived for each line, we stress that the predictions of the observability of redshifted fine-structure lines made in Section 3 must be regarded as tentative and preliminary.

2.3 CO rotational transitions

2.3.1 CO line excitation

Much more observational data is available about the properties of the ladder of CO rotational transitions in the ISM. The energy of the Jth level in the CO molecular rotation ladder $E_J = k_{\rm B}T$, where $T = J(J+1)[2.77\,{\rm K}]$, and so the energy of a photon produced in the $J+1 \rightarrow J$ transition is $h\nu = k_{\rm B}(J+1)[5.54\,{\rm K}]$. The population of the J states can be calculated by assuming a temperature and density for the emitting gas. The primary source of excitation is expected to be collisions with molecular hydrogen (H_2), which dominates the mass of the ISM, with a role for radiative excitation, including that attributable to the cosmic microwave background radiation (CMBR). By taking into account the spontaneous emission rate, $A_{J+1,J} \propto \nu^3(J+1)/(2J+3)$ with $A_{1,0} = 6 \times 10^{-8}\,{\rm s}^{-1}$, and details of the optical depth and geometry of gas and dust in the emitting region, the luminosities of the various $J+1 \rightarrow J$ rotational transitions can be calculated. If the J state is to be thermally populated, then the rate of CO–H_2 collisions in the ISM gas must be greater than about $A^{-1}_{J+1,J}$. This condition will not generally be met for a temperature of 50 K in the CO(5→4) transition unless the density of H_2 molecules exceeds about $2 \times 10^5\,{\rm cm}^{-3}$, which is many times denser than the $10^4\,{\rm cm}^{-3}$ that appears to be typical of low-redshift ULIRGs (Downes & Solomon 1998). Radiative excitation and optical depth effects, perhaps in very non-isotropic geometries, with very pronounced substructure, will complicate the situation greatly in real galaxies. In general, calculations of level populations are very complex, and at high redshifts there are very few data with which to constrain models.

Probably the best way to investigate the conditions in very luminous distant galaxies is to study their low-redshift ULIRG counterparts, and the rare examples of high-redshift galaxies and quasars for which more than one CO transition has been detected (e.g. Downes et al. 1999), bearing in mind the potential effects of gravitational lensing.

In order to try and make reasonable predictions for the line ratios in high-redshift galaxies, we employed a standard large velocity gradient (LVG) analysis (e.g. de Jong, Dalgarno & Chu 1975) to estimate how the CO line ratios are affected by the temperature, density and finite spatial extent of the ISM, and by the radiative excitation caused by the CMBR. In the third column of Table 1 we show the results from this model, assuming a density of $10^4\,{\rm cm}^{-3}$, which is typical of the central regions of ULIRGs (Downes & Solomon 1998), and a standard value of $X({\rm CO})/({\rm d}v/{\rm d}r) = 3 \times 10^{-5}\,({\rm km\,s^{-1}\,pc^{-1}})^{-1}$. We assume a kinetic temperature of 53 K, which is the temperature of the dominant cool dust component in the SCUBA galaxy SMM J02399−0136 (Ivison et al. 1998b). Higher dust temperatures of about 80 and 110 K are inferred for other well-studied high-redshift galaxies *IRAS* F10214+4724 and APM 08279+5255 respectively, but these are very exotic galaxies, and the results are potentially modified by the effects of differential gravitational lensing. We assume a background temperature of 10 K, the temperature of the CMBR at $z = 2.7$, the mean redshift of the two SCUBA galaxies with CO detections. The line-to-continuum bolometric luminosity ratio $f_{\rm line} = L_{J+1\rightarrow J}/L_{\rm FIR}$ can be calculated if the bolometric continuum luminosity $L_{\rm FIR}$ is known. There is a clear trend of a reduction in the CO line-to-bolometric luminosity ratio of luminous infrared galaxies as the bolometric luminosity increases, with a large scatter, which is consistent with $f_{\rm line} \propto L_{\rm FIR}^{-0.5}$ (Sanders et al. 1986). We normalize the results to the observed CO(3→2) line luminosity in the $L_{\rm FIR} \simeq 10^{13}\,{\rm L}_\odot$ SCUBA galaxies SMM J02399−0136 and SMM J14011+0252, in which the ratios of the luminosity in the CO(3→2) line to $L_{\rm FIR}$ is about 2.1×10^{-6} and 5.3×10^{-6} respectively (Frayer et al. 1998, 1999), with errors of order 50 per cent. The dominant source of error is the uncertainty in the bolometric luminosity.

We compare the results obtained in a simple equilibrium case, in which the density of CO molecules, the spontaneous emission rates and the transition energies in different J states are multiplied to give the luminosity in each transition,

$$L_{J+1\rightarrow J} \propto \nu^3 (J+1)^2 \exp\{-[2.77\,{\rm K}](J+1)(J+2)/T\}. \quad (1)$$

The results are shown in the fourth and fifth columns of Table 1 for $J \leq 9$, assuming kinetic temperatures of 38 and 53 K respectively, the temperature generated by simple fits to the observed counts of *IRAS* and *ISO* galaxies (Blain et al. 1999c), and the spectral energy distribution (SED) of SMM J02399−0136.

2.3.2 The effects of different excitation conditions

The values of $f_{\rm line}$ listed in Table 1 for CO transitions in the LVG and the 38- and 53-K thermal equilibrium models differ. However, in lines with $J \lesssim 7$ the differences are less than a factor of a few. Given the current level of uncertainty in the data that support these calculations, this is an acceptable level. The differences between the results are more marked at large values of J. The consequences of these differences for the key predictions of the source counts of line-emitting galaxies are discussed in Section 3.2.

Throughout the paper we use the LVG model to describe the CO line emission of dusty galaxies. Observations of the CO line ratios in low-redshift dusty

Table 1. The fraction of the bolometric luminosity of distant dusty galaxies that is assumed to be emitted in a variety of submillimetre-wave lines $f_{\rm line}$, their restframe emission frequencies $\nu_{\rm rest}$, and the redshifts at which the lines would be detected in the important observing bands at 90, 230, 345 and 650 GHz; z_{90}, z_{230}, z_{345} and z_{650} respectively. The CO ratios $f_{\rm line}$ listed in the third, fourth and fifth columns are calculated assuming the LVG model described in Section 2, and in two local thermal equilibrium models with kinetic temperatures of 38 and 53 K respectively. The fraction of the bolometric luminosity of the galaxies in all CO transitions, obtained by adding all values of $f_{\rm line}$ is also shown. The values of $f_{\rm line}$ listed for fine-structure transitions in the final six rows are derived from observations of low-redshift galaxies and the Milky Way: see Section 2.2. The line styles and thicknesses used to represent the various transitions are listed in the final column.

Line	$\nu_{\rm rest}$ / GHz	$f_{\rm line}$ (LVG)	$f_{\rm line}$ ($T = 38$ K)	$f_{\rm line}$ ($T = 53$ K)	z_{90}	z_{230}	z_{345}	z_{650}	Line style
CO(1→0)	115	1.8×10^{-7}	3.4×10^{-8}	2.8×10^{-8}	0.28	N/A	N/A	N/A	CO lines are represented
CO(2 → 1)	230	1.3×10^{-6}	8.2×10^{-7}	7.2×10^{-7}	1.6	0.0	N/A	N/A	by solid lines whose
CO(3 → 2)	345	4.0×10^{-6}	4.0×10^{-6}	4.0×10^{-6}	2.8	0.50	0.0	N/A	thickness increases with
CO(4 → 3)	461	8.3×10^{-6}	9.6×10^{-6}	1.1×10^{-5}	4.1	1.0	0.34	N/A	the value of J
CO(5 → 4)	576	1.3×10^{-5}	1.4×10^{-5}	2.0×10^{-5}	5.4	1.5	0.67	N/A	
CO(6 → 5)	691	1.6×10^{-5}	1.4×10^{-5}	2.6×10^{-5}	6.7	2.0	1.0	0.06	
CO(7 → 6)	806	1.4×10^{-5}	1.1×10^{-5}	2.8×10^{-5}	8.0	2.5	1.4	0.24	
CO(8 → 7)	922	4.2×10^{-6}	6.8×10^{-6}	2.3×10^{-5}	9.2	3.0	1.7	0.42	
CO(9 → 8)	1040	1.6×10^{-9}	3.3×10^{-6}	1.6×10^{-5}	12	3.5	2.0	0.60	
Total CO	N/A	6.1×10^{-5}	6.6×10^{-5}	1.5×10^{-4}	N/A	N/A	N/A	N/A	N/A
[CII]	1890	10^{-4}	...	...	20	7.2	4.5	1.9	Thick dashed line
$[{\rm CI}]_{809\,{\rm GHz}}$	809	2.9×10^{-5}	...	...	8.0	2.5	1.3	0.24	Thick dot-dashed line
$[{\rm CI}]_{492\,{\rm GHz}}$	492	2.9×10^{-6}	...	...	4.5	1.1	0.43	N/A	Thin dot-dashed line
$[{\rm NII}]_{2460\,{\rm GHz}}$	2460	6.4×10^{-4}	...	...	26	9.6	6.1	2.8	Thick dotted line
$[{\rm NII}]_{1460\,{\rm GHz}}$	1460	4.0×10^{-4}	...	...	15	5.3	4.2	1.2	Thin dotted line
$[{\rm OI}]_{2060\,{\rm GHz}}$	2060	2.4×10^{-4}	...	...	22	8.0	5.0	2.2	Thin dashed line

galaxies indicate a wide range of excitation conditions, $T_{\rm b}[{\rm CO}(3{\rightarrow}2)/{\rm CO}(1{\rightarrow}0)] \sim 0.2$–1 (Mauersberger et al. 1999). In the central regions of starburst nuclei this temperature ratio tends to be systematically higher, with $T_{\rm b}[{\rm CO}(3{\rightarrow}2)/{\rm CO}(1{\rightarrow}0)] \simeq 0.5$–1 (Devereux et al. 1994). In our chosen LVG model, listed in Table 1, this ratio is $\simeq 0.9$, which is consistent with the observations of the central regions of M82 (Wild et al. 1992) and Arp 220 (Mauersberger et al. 1999). The value of the X parameter in the model has little effect on these ratios; however, reducing the density from 10^4 to 3300 and 1000 cm^{-3} reduces the predicted ratio to 0.81 and 0.51 respectively. Our model looks reasonable in the light of these observations, as the high-redshift galaxies would typically be expected to be ULIRGs with high gas densities.

There have been two recent discussions of the observability of CO line emission from high-redshift galaxies. Silk & Spaans (1997) describe the effect of the increasing radiative excitation of high-J lines at very high redshifts because of the increasing temperature of the CMBR. The median redshift of the SCUBA galaxies is likely to be about 2–3 (Barger et al. 1999b; Smail et al. 2000; Lilly et al. 1999), with perhaps 10–20 per cent at $z \gtrsim 5$, and because there is currently no strong evidence for the existence of a large population of metal-rich galaxies at $z \gtrsim 10$, this effect is unlikely to be very important. Combes et al. (1999) include a hot dense 90-K/10^6 cm^{-3} component in the ISM of their model high-redshift galaxies, in addition to the cooler less dense component included in our models, and conduct LVG calculations to determine CO emission-line luminosities. Understandably, the luminosity of high-J CO lines is predicted to be greater in their models as compared with the values listed in Table 1. The continuum SED of the best studied SCUBA galaxy SMM J02399−0136 certainly includes a contribution from dust at temperatures greater than 53 K, but here we avoid including additional hot dense phases of the ISM in our models in order to avoid complicating the models and to try and make conservative predictions for the observability of high-J CO lines at high redshift.

Only additional observations of CO in high-redshift galaxies will allow us to improve the accuracy of the conditions in the ISM that are assumed in these models. The detection of the relative intensities of the CO(9→8) and CO(5→4) emission from APM 08279+5255 (Downes et al. 1999), and the ratio of the intensities of the multiple CO lines detected in BR 1202−0725 at $z = 4.7$ (Ohta et al. 1996, 1998; Omont et al. 1996) are broadly consistent with the values of $f_{\rm line}$ listed in the 53-K thermal equilibrium model: see Table 1.

The evolution of the abundance of CO and dust throughout an episode of star formation activity have been investigated by Frayer & Brown (1997), and the detailed appearance of the submillimetre-wave emission-line spectrum of galaxies requires a careful treatment of the radiative transfer between stars, AGN, gas and dust in an appropriate geometry. However, given that the amount of information on the spectra of high-redshift galaxies is currently not very great, it seems sensible to base estimates of the properties of line emission on the template of the submillimetre-selected galaxies studied by Frayer et al. (1998, 1999).

2.3.3 Other molecular emission lines

There could also be a contribution from rotational lines emitted by other species, such as NH_3, CS, HCN, HCO^+ and H_2O; however, it seems unlikely that these emission lines would dominate the energy emitted in CO unless the densities and excitation temperatures are very high.

2.4 High-redshift dusty galaxies

The surface density of 850-μm SCUBA galaxies is now known reasonably accurately between flux densities of 1 and 10 mJy (Barger et al. 1999a; Blain et al. 1999b, 2000). By combining knowledge of the properties of the SCUBA galaxies, the low-redshift 60-μm *IRAS* galaxies (Saunders et al. 1990; Soifer & Neugebauer 1991), the 175-μm *ISO* galaxies (Kawara et al. 1998; Puget et al. 1999) and the intensity of far-infrared background radiation (Fixsen et al. 1998; Hauser et al. 1998; Schlegel, Finkbeiner & Davis 1998), it is possible to construct a series of self-consistent models that can account for all these data (Guiderdoni et al. 1998; Blain et al. 1999b,c), under various assumptions about the formation and evolution of galaxies. The 'Gaussian' model, which is described by Blain et al. (1999b) and based on pure luminosity evolution of the low-redshift 60-μm luminosity function (Saunders et al. 1990), was modified slightly to take account of the tentative redshift distribution derived from the SCUBA lens survey by Barger et al. (1999b). This 'modified Gaussian' model is used as a base for the predictions of line observability presented here. The evolution function increases as $(1+z)^\gamma$ with $\gamma \simeq 4$ at $z \lesssim 1$, has a 1.0-Gyr-long Gaussian burst of luminous activity centred at $z = 1.7$, in which L^* is 70 times greater than the value of L^* at $z = 0$ (Saunders et al. 1990), and then declines at $z \gtrsim 3$.

This model contains fewer parameters than there are constraining pieces of information, and so should provide a reasonable description of the properties of high-redshift dust-enshrouded galaxies, which are expected to be the most easily detectable sources of line emission. Future observations will inevitably provide more information and demand modifications to the model of galaxy evolution discussed above; however, it is likely to provide a sound basis for the predictions below.

3 LINE PREDICTIONS

In this paper we are concerned with the detectability of redshifted lines rather than with their resolution. As a result, we want to estimate the total luminosity of a line, and will not be concerned with details of its profile. The results are all presented as integrated flux densities, determined over the whole line profile. Where relevant, a line width of 300 km s^{-1} is assumed.

The evolution of the 60-μm luminosity function of dusty galaxies (Saunders et al. 1990) is assumed to be defined by the modified Gaussian model. The bolometric far-infrared continuum luminosity function $\Phi_{\rm bol}(L_{\rm FIR})$ can then be calculated by integrating over a template dusty galaxy SED (Blain et al. 1999b). $\Phi_{\rm bol}$ can in turn be converted into a luminosity function for each line listed in Table 1, $\Phi_{\rm line}(L_{\rm line}, z)$, by evaluating $\Phi_{\rm bol}$ at the bolometric luminosity $L_{\rm FIR}$ that corresponds to the line luminosity $L_{\rm line}$.

Based on observations by Sanders et al. (1986), the ratio of the luminosity in the CO(1→0) line, $L_{\rm CO}$, to $L_{\rm FIR}$ is a function of $L_{\rm FIR}$, with $L_{\rm CO} \propto L_{\rm FIR}^{0.5}$. Hence, when making the transformation from $L_{\rm line}$ to $L_{\rm FIR}$ for the CO lines listed in Table 1, we use the relationship $L_{\rm FIR} = L_{\rm line}/f_{\rm line}$, in which $f_{\rm line} \propto L_{\rm FIR}^{-0.5}$ and is normalized to the value listed in Table 1 at 10^{13} L$_\odot$, the luminosity of the submillimetre-selected galaxies SMM J02399−0136 and SMM J14011+0252. There is no evidence from *ISO* observations of any systematic luminosity dependence in the value of $f_{\rm line}$ for [CII] emission from ULIRGs, and so we assume that the values of $f_{\rm line}$ listed in Table 1 describe the line-to-bolometric luminosity relation in the fine-structure lines at all luminosities, that is $L_{\rm FIR} = L_{\rm line}/f_{\rm line}$, where $f_{\rm line}$ is constant.

The surface density of line-emitting galaxies $N(>S)$ that can be detected at integrated flux densities brighter than S, as measured in Jy km s^{-1} or W m^{-2}, in an observing band spanning the frequency range between $\nu_{\rm obs}$ and $\nu_{\rm obs} + \Delta\nu_{\rm obs}$ can be calculated by integrating the luminosity function of a line $\Phi_{\rm line}$ over the redshifts for which the line is in the observing band, and luminosities $L_{\rm line}$ greater than the detection limit $L_{\rm min}(S, z)$. The count of galaxies is thus

$$N(>S) = \int_{z_1}^{z_2} \int_{L_{\rm min}(S,z)}^{\infty} \Phi_{\rm line}(L_{\rm line}, z)\, {\rm d}L_{\rm line}\, D^2(z) \frac{{\rm d}r}{{\rm d}z}\, {\rm d}z. \quad (2)$$

D is the comoving distance parameter to redshift z, and dr is the comoving distance element. For a line with a restframe emission frequency $\nu_{\rm line}$, the limits in equation (2) are

$$z_1 = \frac{\nu_{\rm obs} + \Delta\nu_{\rm obs}}{\nu_{\rm line}} - 1, \quad (3)$$

and

$$z_2 = \frac{\nu_{\rm obs}}{\nu_{\rm line}} - 1. \quad (4)$$

If $z_1 \geq z_0$, where z_0 is the maximum redshift assumed for the galaxy population, or if $z_2 \leq 0$, then the count $N = 0$. Here $z_0 = 10$ is assumed. The minimum detectable line luminosity,

$$L_{\rm min}(S, z) = 4\pi S D^2 (1+z)^2. \quad (5)$$

If the integrated flux density of a line S observed at frequency ν, is 1 W m^{-2}, then the same quantity can be expressed as $3(\nu/{\rm Hz})^{-1} \times 10^{31}$ Jy km s^{-1}.

The counts calculated for the transitions listed in Table 1 are shown in Figs 1–3. Predictions are made at centre frequencies (bandwidths) of 23 (8) – the radio K band, 50 (8) – the radio Q band, 90 (1), 230 (8), 345 (8), 650 (8), 200 (100) GHz, and 1 (1) THz, in Figs 2(a), 2(b), 1(a), 1(b), 1(c), 1(d), 3(a) and 3(b) respectively. The 8-GHz radio bandwidth is matched to the performance specified for the upgraded VLA. The 1-GHz bandwidth at 90 GHz is approximately matched to the current performance of millimetre-wave interferometer arrays. The 8-GHz bandwidth at 230, 345 and 650 GHz matches that for the SPIFI Fabry–Perot spectrograph (Stacey et al. 1996; Bradford et al. 1999, in preparation) and is a plausible value for the bandwidth of the future ground-based Atacama Large Millimetre Array (ALMA; Ishiguro et al. 1994; Brown et al. 1996; Downes et al. 1996), although the current goal is for a 16-GHz bandwidth (Wootten 2000). The count predictions in the very

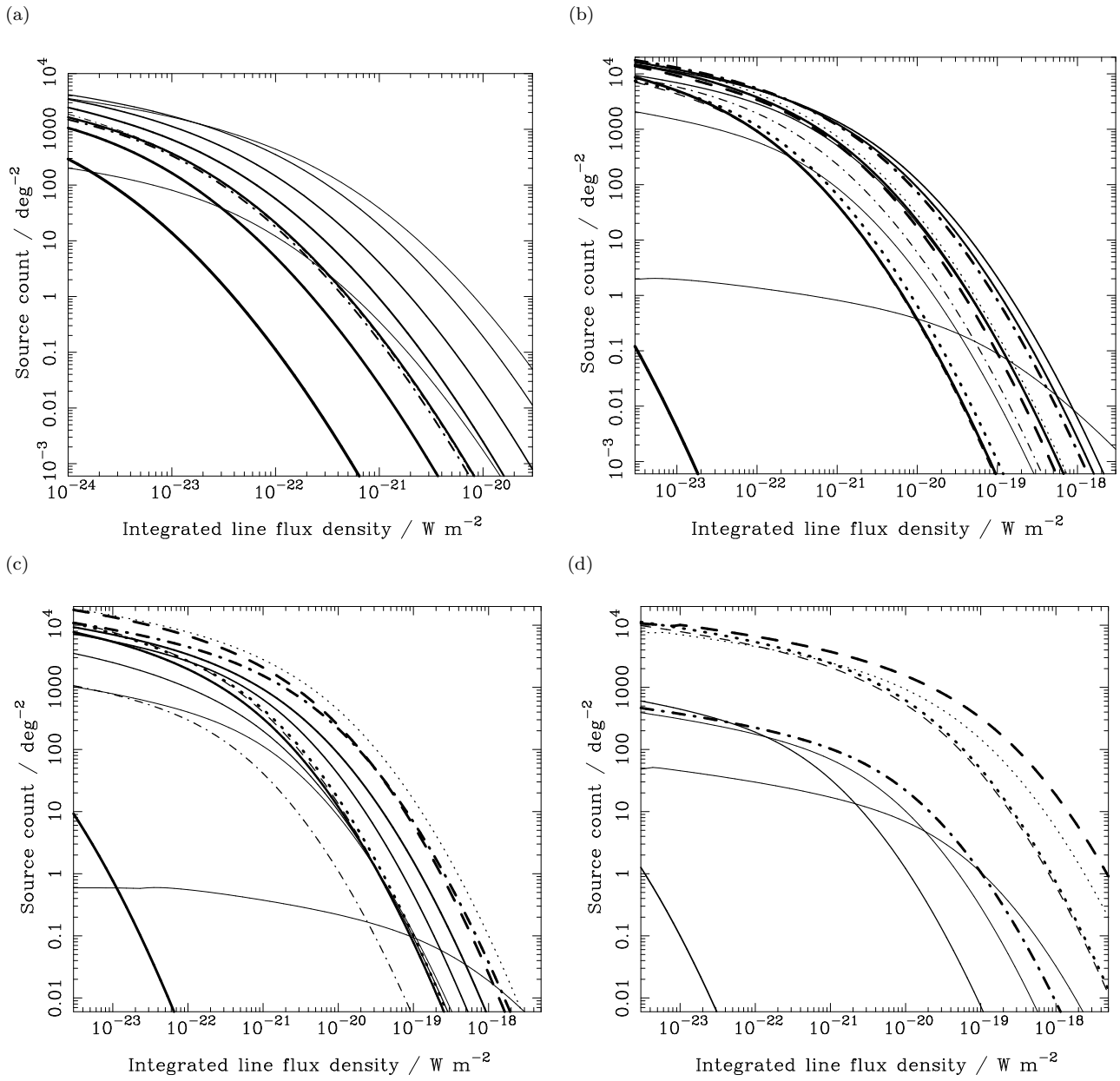

Figure 1. Predicted counts of CO rotation and fine-structure lines detectable from galaxies in a 1-GHz band centred at 90 GHz (a), and in 8-GHz bands centred on (b) 230 GHz, (c) 345 GHz and (d) 650 GHz. The band in (a) is accessible to the existing BIMA, IRAM, Nobeyama and OVRO interferometer arrays. These arrays also operate with a narrower 1-GHz bandwidth around 230-GHz (b). ALMA will operate in all the bands shown in (b), (c) and (d), with a current goal bandwidth of 16 GHz (Wootten 2000). SPIFI and the HIFI and SPIRE-FTS instruments on the *FIRST* satellite will operate in the band shown in (d). The line styles and thicknesses correspond to each transition listed in Table 1. In (a) the CO rotational transitions from CO(1→0) to CO(8→7) and the [CI]$_{492\,\mathrm{GHz}}$ line are present, in (b) CO(2→1) to CO(9→8) and all the fine-structure lines listed in Table 1 are detectable, in (c) CO(3→2) to CO(9 →8) and all the fine-structure lines are present, and in (d) the CO transitions from CO(6→5) to CO(9→8) and all but the [CI]$_{492\,\mathrm{GHz}}$ fine-structure line are present. $10^{-20}\,\mathrm{W\,m^{-2}}$ is equivalent to 3.3, 1.3, 0.9 and 0.5 Jy km s^{-1} at 90, 230, 345 and 650 GHz respectively.

wide atmospheric window between 150 to 250 GHz is shown in Fig. 3(a). This band cannot be observed simultaneously using heterodyne instruments, but could plausibly be covered using an advanced grating or Fabry–Perot spectrograph feeding a sensitive bolometer detector array. In Fig. 3(b) the far-infrared/submillimetre band between 460 and 1500 GHz is shown. This band is matched to the specified spectral range of the SPIRE Fourier Transform Spectrograph destined for the *FIRST* satellite (Griffin 1997; Griffin et al. 1998).

3.1 The shape of the counts and optimal surveys

The integrated counts, $N(>S) \propto S^{-\alpha}$ presented in Figs 1 to 3 all have a characteristic form, with a relatively flat slope, $\alpha \simeq 0.3$, at faint flux densities, which rolls over to

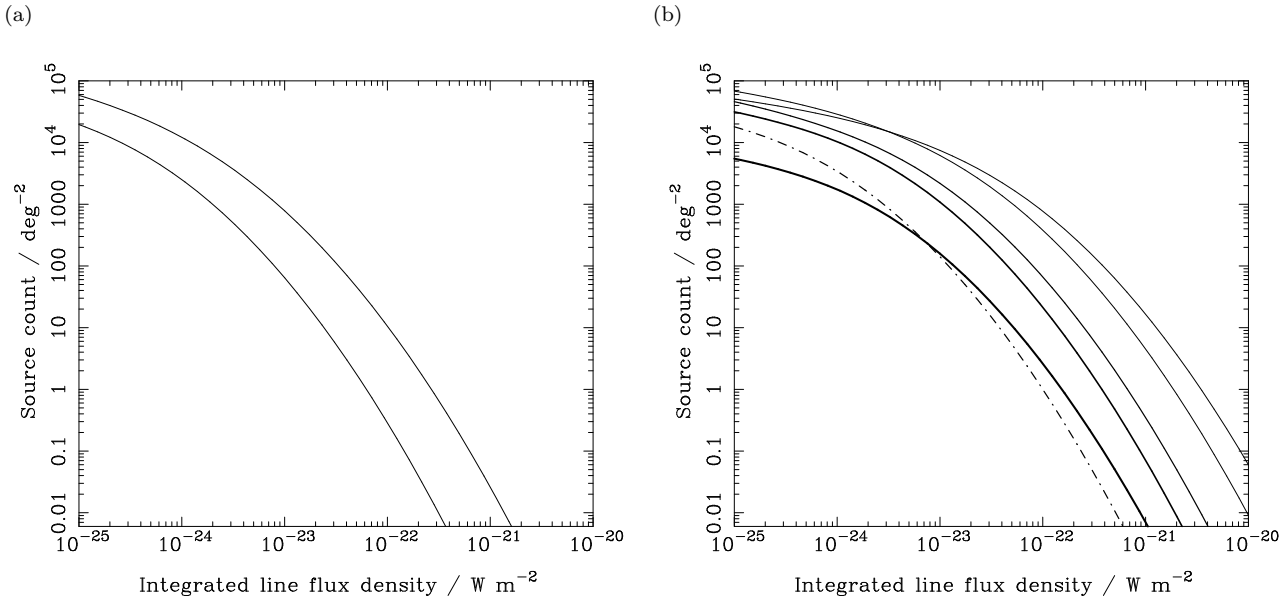

Figure 2. The line counts for galaxies at $z < 10$ predicted in a 8-GHz band centred at (a) 23 GHz and (b) 50 GHz, corresponding to the K and Q bands. In (a) only the CO(1→0) and CO(2→1) lines are redshifted into the band. In (b) CO lines up to CO(5→4) and the $[\mathrm{CI}]_{492\,\mathrm{GHz}}$ line are present. The line styles and thicknesses that correspond to the transitions are listed in Table 1. $10^{-22}\,\mathrm{W\,m^{-2}}$ is equivalent to 0.13 and 0.06 Jy km s^{-1} at 23 and 50 GHz respectively.

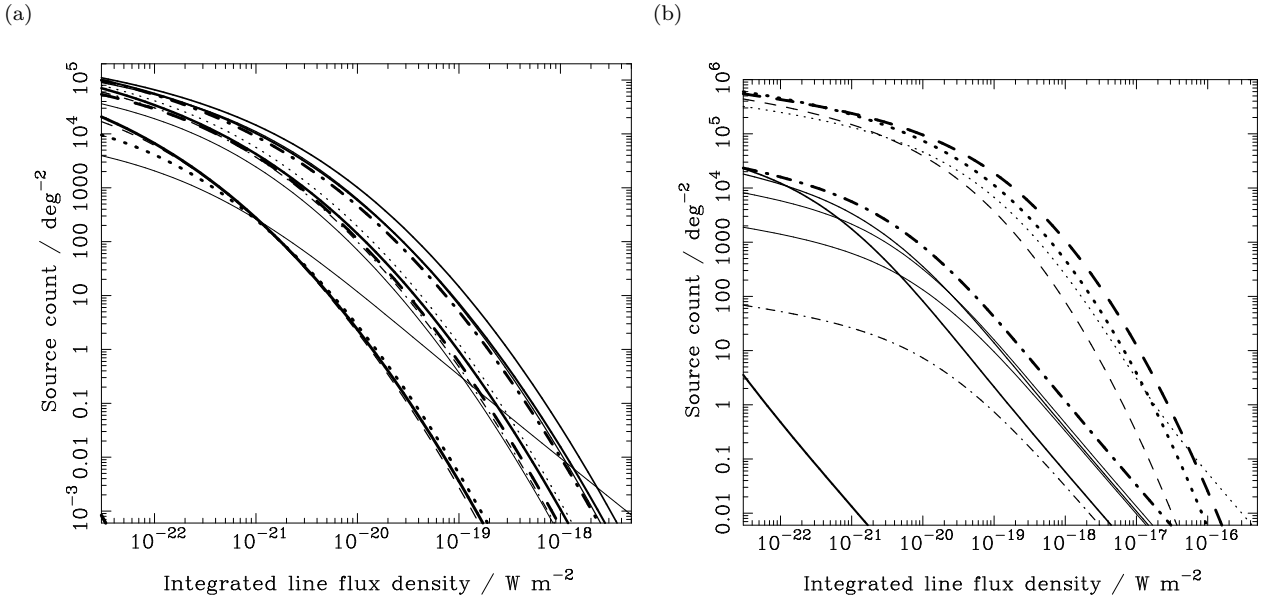

Figure 3. The line counts predicted in very wide bands covering the spectral ranges between 150–250 GHz (a) and 460–1500 GHz (b). The band in (a) could be observed using a grating spectrograph feeding bolometer detectors. The band in (b) could be surveyed using the SPIRE-FTS instrument fitted to *FIRST*. The lowest CO transition shown in (a) is CO(2→1). In (b) the lowest CO transition is CO(5→4), and the counts are dominated by fine-structure lines. The line styles and thicknesses that correspond to each transition are listed in Table 1. $10^{-20}\,\mathrm{W\,m^{-2}}$ is equivalent to 1.5 and 0.4 Jy km s^{-1} at 200 and 800 GHz respectively.

a steep decline, $\alpha \simeq 3$, at brighter fluxes. Note that the detection rate of galaxies in a survey is maximized at the depth at which $\alpha = 2$. Because the counts of lines presented here have a pronounced knee at a certain flux density, at which the value of α crosses 2, this flux density is the optimal depth for a blank-field line survey, and surveys that are either shallower or deeper should be much less efficient.

In Fig. 4 the predicted counts of line-emitting galaxies are shown as a function of observing frequency between 50 and 2000 GHz, at both faint and relatively bright values of the integrated line flux density S, 10^{-22} and $10^{-20}\,\mathrm{W\,m^{-2}}$. The form of the curve for each emission line is determined by the form of evolution of far-infrared luminous galaxies specified in the modified Gaussian model. In any particular line, galaxies detected at higher frequencies are at lower redshifts. This effect accounts for the double-peaked distribution that is most apparent in the counts of bright galaxies shown in Fig. 4(b). The broad peak at lower frequencies cor-

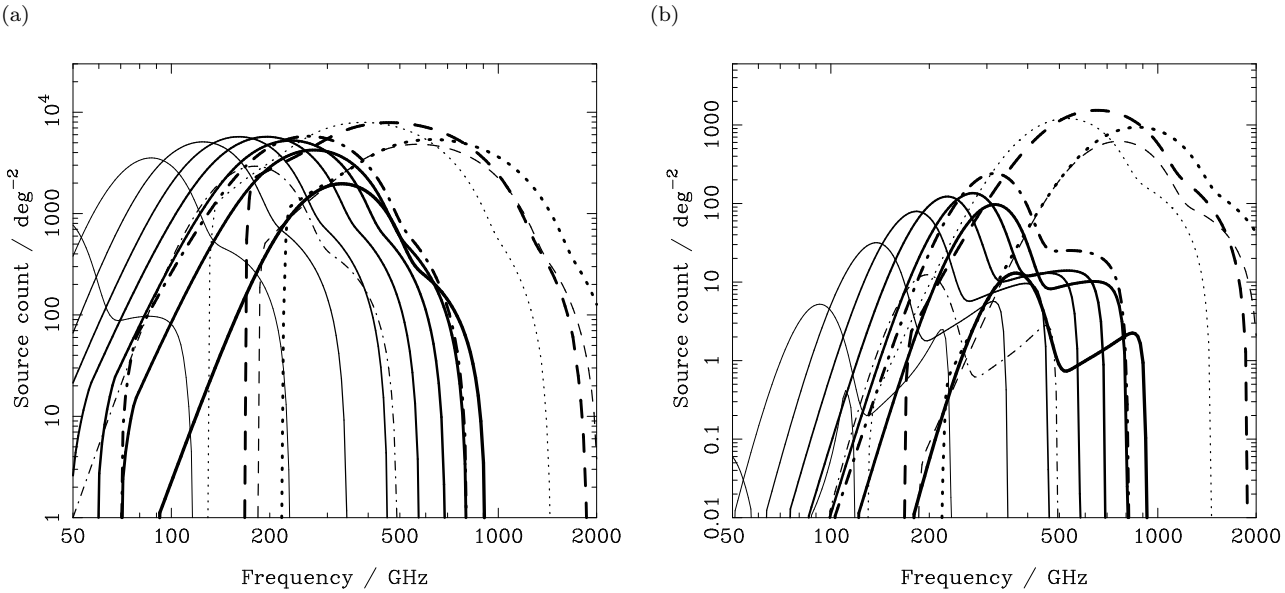

Figure 4. The surface density of line emitting galaxies brighter than (a) $10^{-22}\,\mathrm{W\,m^{-2}}$ and (b) $10^{-20}\,\mathrm{W\,m^{-2}}$, as a function of observing frequency, assuming an observing bandwidth of 8 GHz. The line styles are listed in Table 1. The sharp lower cutoff to the counts of fine-structure lines at low frequencies is attributable to the assumed upper limit to the redshift distribution of dusty galaxies, $z_0 = 10$. If gas-rich galaxies exist at $z > 10$, then they would be detectable at frequencies below these cutoffs.

responds to the very luminous Gaussian burst of activity at $z \simeq 1.7$, while less luminous low-redshift galaxies account for the second sharper peak at higher frequencies. The double peak is more noticeable for the brighter counts, to which the contribution of low-redshift galaxies is more significant.

Based on the predicted counts of CO lines, which are probably quite reliable, the most promising frequency range in which to aim for CO line detections is 200–300 GHz, regardless of whether faint or bright CO lines are being sought. At frequencies greater than about 500 GHz the counts are expected to be dominated by fine-structure lines, and although these counts are still very uncertain, the detectability of fine-structure line emitting galaxies is expected to be maximized at a frequency between about 400 and 800 GHz. Future blank-field searches for fine-structure emission from distant galaxies should probably be concentrated in this range.

3.2 The effects of CO excitation

The three different sets of values of f_{line} listed for CO transitions in Table 1 were derived assuming different excitation conditions in the ISM. As the detailed astrophysics of gas-rich high-redshift galaxies is very uncertain and only weakly constrained by observations, there is an inevitable uncertainty in the counts predicted in Figs 1–4.

The most significant differences between the values of f_{line} predicted in the LVG, 38-K and 53-K models occur in the higher J lines, for which the effect of the higher excitation temperature and the subthermal excitation of lines in the LVG model is greater. The increase is most significant at bright flux densities. If the alternative values of f_{line} listed in the thermal equilibrium models are used to predict counts similar to those in Figs 1–4, then for $J \leq 7$, at interesting line flux densities of about $10^{-22}\,\mathrm{W\,m^{-2}}$, the counts differ by less than a factor of about 3. This uncertainty is greater than that in the surface density of high-redshift submillimetre-selected galaxies that were used to normalize the model of galaxy evolution, and so the counts predicted in Figs 1–4 should be reliable to within a factor of about 3. Note that the counts in Fig. 4 indicate that the CO(5→4) line is likely to be provide the most significant contribution to the counts, and so the degree of excitation of lines with $J \geq 7$ is not likely to affect the detection rate in future blank-field line surveys.

3.3 The effects of cosmology

In Fig. 5 the 230-GHz counts expected in three different world models are compared, based on the same underlying population of distant dusty galaxies. In world models with $\Omega_0 = 0.3$ and either $\Omega_\Lambda = 0.0$ or 0.7 the faint counts are expected to be greater, and the bright counts are expected to be less, as compared with the predictions of an Einstein–de Sitter model. The count changes as a function of cosmology by a factor of about 10 in the most abundant lines over the wide range of flux densities presented in Fig. 5, which correspond to a range of count values between about 10^4 and $10^{-3}\,\mathrm{deg^{-2}}$. At a flux density of $10^{-20}\,\mathrm{W\,m^{-2}}$, which is likely to be similar to the limiting depth of future submillimetre-wave line surveys, the counts are modified by only a factor of about 2 by changing the world model. Hence, at present the uncertainties in the excitation conditions in the ISM are expected to be greater than those introduced by uncertainties in the cosmological parameters.

4 LINE OBSERVATIONS

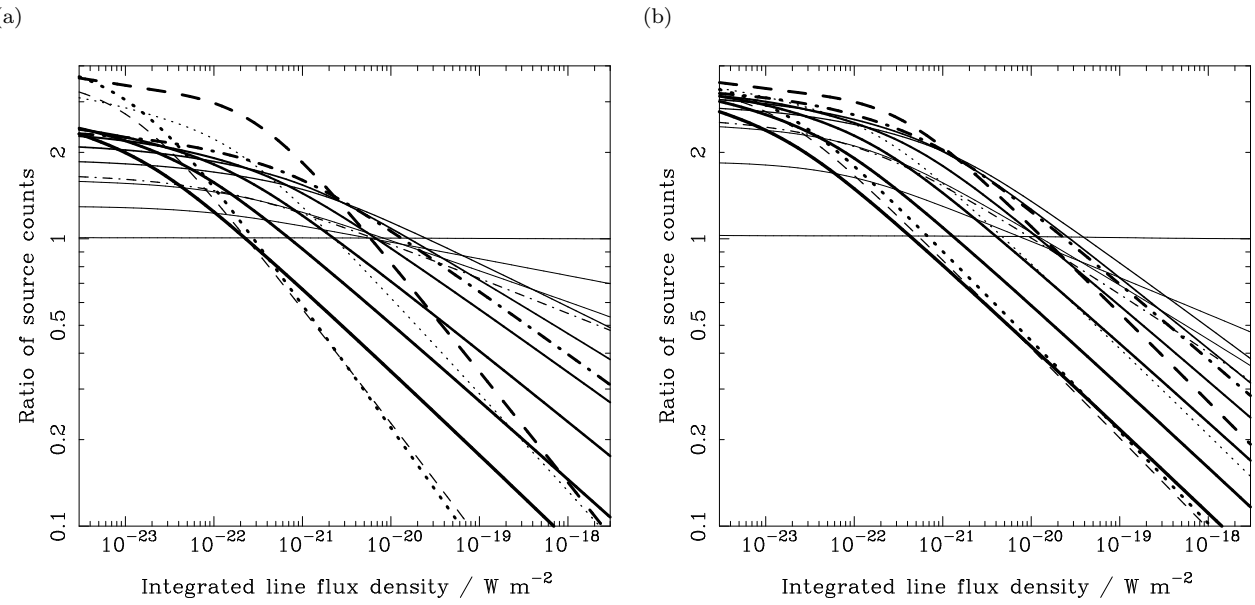

Figure 5. The effects of different world models on the predictions of CO and fine-structure line counts, for demonstration in a narrow band centred on 230 GHz (see Fig. 2). The line styles and thicknesses that correspond to each transition are listed in Table 1. The results are presented as ratios between the counts in two world models with $\Omega_0 < 1$, and the predictions of an Einstein–de Sitter model. In (a) the cosmological parameters are $\Omega_0 = 0.3$ and $\Omega_\Lambda = 0.0$; in (b) $\Omega_0 = 0.3$ and $\Omega_\Lambda = 0.7$. The differences due to the world model are by factors of a few, at worst comparable with the level of uncertainty in the count predictions that is attributable to the uncertain excitation conditions in the ISM.

4.1 Millimetre-wave interferometer arrays

Four millimetre-wave interferometer arrays are currently operating: the BIMA array with ten 6-m antennas; the IRAM array with five 15-m antennas; the Nobeyama Millimeter Array with six 10-m antennas; and the OVRO Millimeter Array with six 10.4-m antennas. These instruments operate at wavelengths longer than 1 mm, and their fields of view and sensitivities translate into similar mapping speeds to equivalent flux density levels. For example, in a 20-hr integration at a frequency of 90 GHz, the OVRO Millimeter Array is able to reach a 5σ sensitivity limit of about $5 \times 10^{-21}\,\mathrm{W\,m^{-2}}$ across a 1-GHz band in a 1-arcmin^2 primary beam.

The counts of lines expected in a 90-GHz observation with a 1-GHz bandwidth are shown in Fig. 1(a) as a function of integrated line flux density. At this limiting flux density, a count of about $2\,\mathrm{deg^{-2}}$ is expected, and so the serendipitous detection of an emission line in a blank-field survey would be expected to occur after approximately 4×10^4 hr. In 230-GHz observations with the same 1-GHz bandwidth, which are possible in good weather, the sensitivity required for a 5σ detection in a 20-h integration is about $2 \times 10^{-20}\,\mathrm{W\,m^{-2}}$, in a 0.25-arcmin^2 primary beam. The 230-GHz count expected at this depth, after correcting the results shown in Fig. 1(b) for the narrower bandwidth, is about $50\,\mathrm{deg^{-2}}$. A serendipitous line detection would thus be expected about every 6000 hr. Thus, while known high-redshift galaxies can certainly be reliably detected in reasonable integration times using these arrays, blank-field surveys for emission lines are not currently practical.

The detection of redshifted CO lines at a 90-GHz flux density of about $10^{-20}\,\mathrm{W\,m^{-2}}$ from two submillimetre-wave continuum sources, with a surface density of several $100\,\mathrm{deg^{-2}}$ (Blain et al. 1999b, 2000), using the OVRO array (Frayer et al. 1998, 1999) is consistent with the 90-GHz line count of about $2\,\mathrm{deg^{-2}}$ predicted in Fig. 1(a) at this flux density. This is because observations in many tens of 1-GHz bands would have been required to search for a CO emission line from these galaxies without an optical redshift, and so the source count of lines at the detected flux density is expected to be about two orders of magnitude less than that of the dust continuum-selected galaxies.

The large ground-based millimetre/submillimetre-wave interferometer array ALMA will provide excellent subarcsecond angular resolution and a large collecting area for observations of submillimetre-wave continuum and line radiation. Based on the performance described for ALMA at 230 GHz by Wootten (2000), a 300-km-s^{-1} line with an integrated flux density of $5 \times 10^{-22}\,\mathrm{W\,m^{-2}}$ could be detected at 5σ significance, but not resolved, anywhere within a 16-GHz band in about 1 hr in the 0.15-arcmin^2 primary beam. The surface density of lines brighter than this flux density is expected to be about $2.5 \times 10^4\,\mathrm{deg^{-2}}$ (Fig. 1b; see also Blain 2000), and so a detection rate of about $1.7\,\mathrm{hr^{-1}}$ would be expected. The knee in the counts in Fig. 1(b), indicating the most efficient survey depth, is at a flux density greater than about $10^{-20}\,\mathrm{W\,m^{-2}}$, a depth reached in an integration time of about 10 s at 5σ significance. Hence, making a large mosaic map at this depth, covering an area of $0.017\,\mathrm{deg^2\,hr^{-1}}$ should maximize the detection rate, which would then be about 15 galaxies per hour, neglecting scanning overheads incurred in the mosaiking process. This detection rate would allow large samples of line-emitting high-redshift galaxies to be compiled rapidly using ALMA. The performance of ALMA in line searches is discussed in more detail by Blain (2000).

4.2 Ground-based single-antenna telescopes

At present the heterodyne spectrographs fitted to the JCMT, the Caltech Submillimeter Observatory (CSO), and the IRAM 30-m antenna are not sufficiently sensitive to allow a blank-field survey to search for distant line emitting galaxies. For example, the 230-GHz receiver at the JCMT, which is the least susceptible to atmospheric noise, can reach a 5σ sensitivity of about $2 \times 10^{-19}\,\mathrm{W\,m^{-2}}$ in a 1-hr observation in a 1.8-GHz band centred on 230 GHz. At this flux density the surface density of CO line emitting galaxies is expected to be $\lesssim 10\,\mathrm{deg^{-2}}$ (see Fig. 1b), and so because the beam area is $2.4 \times 10^{-5}\,\mathrm{deg^2}$, many tens of thousands of hours of observation would be required to detect a source serendipitously. The development of wide-band correlators, such as the 3.25-GHz WASP (Isaak, Harris & Zmuidzinas 1999), will improve the performance of single-antenna telescopes significantly for the detection of faint lines in galaxies with a known redshift, but unless bandwidths are increased by at least an order of magnitude, blank-field line searches from the ground will not be practical.

4.2.1 Future instrumentation

At present, submillimetre-wave emission lines from a particular distant galaxy can only be detected if an accurate redshift has been determined, because the instantaneous bandwidth of receivers is narrow, and accurate tuning is required for a target line to be observed within the available band. For galaxies and AGN detected in blank-field submillimetre continuum surveys, obtaining a spectroscopic redshift requires a very considerable investment of observing time (see, e.g., Smail et al. 1999a). However, if a much wider bandwidth of order $115\,\mathrm{GHz}/(1+z)$ could be observed simultaneously, then a CO line would always lie within the observing band from a galaxy at redshift z.

There are currently two ways to increase the instantaneous bandwidth of a ground-based millimetre-wave telescope, both based on bolometer detectors rather than heterodyne mixers. Either a resonant cavity, such as a Fabry–Perot, or a diffraction grating could be used to feed an array of bolometer detectors. The potential of such instruments are discussed in the subsections below.

4.2.2 A Fabry–Perot device: SPIFI

SPIFI is a 5×5 element Fabry-Perot interferometer, for use at frequencies from 460 to 1500 GHz on both the 1.7-m AST-RO telescope at the South Pole and the 15-m JCMT (Stacey et al. 1996; Bradford et al. 1999, in preparation). On AST-RO, in the 350-μm (850-GHz) atmospheric window, the field of view of the instrument is about $25\,\mathrm{arcmin^2}$. At a coarse 300-km-s^{-1} resolution, a bandwidth of about 8 GHz can be observed to a 5σ detection threshold of about $3.2 \times 10^{-17}\,\mathrm{W\,m^{-2}}$ in a 1-hr integration. On the 15-m JCMT, at the same frequency and for the same bandwidth, the field of view and the 5σ detection threshold are both less, about $0.3\,\mathrm{arcmin^2}$ and $8 \times 10^{-19}\,\mathrm{W\,m^{-2}}$ respectively.

From Fig. 1(d), the count at flux densities brighter than the 5σ detection threshold for the JCMT are expected to be about $30\,\mathrm{deg^{-2}}$, and to be dominated by [CII]-emitting galaxies, for which the counts are very uncertain. Hence a serendipitous detection would be expected about every 400 hr, and so blank-field line surveys using SPIFI are on the threshold of being practical. A second-generation instrument with a wider field of view should be capable of making many detections in a reasonable integration time.

4.2.3 A millimetre-wave grating spectrograph

An alternative approach to obtaining a wide simultaneous bandwidth would be to build a grating spectrograph to disperse the signal from a 10-m ground-based telescope onto linear arrays of bolometers. Such an instrument would be able to observe a reasonably large fraction of the clear 150–250 GHz atmospheric window simultaneously, at a background-limited 1σ sensitivity of about $10^{-20}\,\mathrm{W\,m^{-2}}$ in a 1-hr observation, which is uniform to within a factor of about two across this spectral range. The predicted counts of lines in this spectral range are of order $100\,\mathrm{deg^{-2}}$ at this depth (Fig. 3a), and are expected to be dominated by CO lines, for which the predicted counts should be reasonably accurate. At 200 GHz the field of view of a 10-m telescope is about $0.2\,\mathrm{arcmin^2}$, and so a 5σ detection rate of about $0.05\,\mathrm{hr^{-1}}$ would be expected in a blank-field line survey. A grating instrument with these specifications is thus on the threshold of being useful for conducting such a survey.

It would also be very valuable for detecting CO lines emitted by the high-redshift galaxies detected in dust continuum surveys whose positions are known to within about 10 arcsec. An instantaneous bandwidth of order 100 GHz would accommodate either 2 or 3 CO lines for a $z > 2$ galaxy, and so a spectroscopic redshift could be determined without recourse to radio, optical or near-infrared telescopes. For example, the $z = 2.8$ SCUBA galaxy SMM J02399−0136 has an integrated flux density of $1.5 \times 10^{-21}\,\mathrm{W\,m^{-2}}$ in the CO(3→2) transition (Frayer et al. 1998), and all the CO(J+1→J) transitions with J=5, 6, 7 and 8 fall within the 150–250 GHz spectral range. Based on the LVG model (Table 1), these lines are expected to have integrated flux densities of 3.0, 3.6, 3.2 and $1.0 \times 10^{-20}\,\mathrm{W\,m^{-2}}$ respectively. Thus, in a 5-hr integration in the field of SMM J02399−0136, all but the CO(8→7) line could be detected using a background-limited grating spectrograph, allowing its redshift to be determined unequivocally in a comparable time to that required to obtain an optical redshift using a 4-m telescope (Ivison et al. 1998b). There are two further advantages. First, the CO-line redshift would be the redshift of cool gas in the ISM of the galaxy, and not that of optical emission lines, which are typically blueshifted by several $100\,\mathrm{km\,s^{-1}}$ with respect to the ISM. Secondly, the ratios of the luminosities of the detected CO lines would reveal information about the physical conditions in the cool ISM where star-formation takes place.

4.3 Ground-based centimetre-wave telescopes

Low-J CO lines are redshifted into the centimetre waveband for redshifts $z < 10$. Instruments operating in this waveband include the VLA and the Green Bank Telescope (GBT).

Currently, the VLA can observe spectral lines in a very narrow 87.5-MHz band, centred in the K band (22–24 GHz) and Q band (40–50 GHz). In the K band, Ivison et al. (1996)

attempted to detect CO(1→0) emission from the environment of a dusty radio galaxy at $z = 3.8$, and in 12 hours they obtained a 5σ upper limit of about $4 \times 10^{-23}\,\mathrm{W\,m^{-2}}$ in a 2-arcmin beam. Because of the very narrow bandwidth, the detection rate of CO line-emitting galaxies with the K-band VLA in a blank-field survey is expected to be about $1\,\mathrm{yr^{-1}}$. However, by 2002 fibre-optic links and a new correlator will be installed, increasing the simultaneous bandwidth greatly to 8 GHz, and improving the 5σ sensitivities to 1.3×10^{-23} and $8.0 \times 10^{-23}\,\mathrm{W\,m^{-2}}$ in 12-hr K- and Q-band integrations respectively. The counts of line-emitting galaxies at $z \leq 10$ in these bands are shown in Fig. 2. At these sensitivities, K- and Q-band counts of about 500 and $2000\,\mathrm{deg^{-2}}$ are expected respectively, each corresponding to a detection rate of about $0.03\,\mathrm{hr^{-1}}$. The knee in the counts at which the detection rate is maximized is expected at rather similar flux densities of about 3×10^{-23} and $2 \times 10^{-22}\,\mathrm{W\,m^{-2}}$ in the K and Q bands respectively, depths which can be reached in about 140- and 190-min integrations and at which the counts are expected to be about 100 and $400\,\mathrm{deg^{-2}}$ respectively. The most efficient detection rates in the K and Q bands are thus expected to be about 0.04 and $0.03\,\mathrm{hr^{-1}}$. Hence, low-J blank-field CO-line surveys will be practical using the upgraded VLA. High-redshift galaxies with luminosities comparable to the SCUBA galaxies detected by Frayer et al. (1998, 1999) should be readily detectable, as their integrated flux densities in the CO(1→0) line would be of order 7×10^{-23} and $4 \times 10^{-22}\,\mathrm{W\,m^{-2}}$ when redshifted into the K and Q bands, from $z = 4$ and 1.3 respectively.

The 100-m clear-aperture GBT will operate with a 3.2-GHz bandwidth in the K and Q bands, reaching 5σ sensitivity limits in 1-hr integrations of about 1.3 and $5 \times 10^{-22}\,\mathrm{W\,m^{-2}}$ respectively. These sensitivities make the GBT even more suitable for detecting low-J CO lines from known high-redshift galaxies than the VLA, but the subarcminute field of view of the GBT is too small to allow a practical blank-field survey. At these sensitivity limits, only 2×10^{-5} and 6×10^{-4} lines per beam are expected in the K and Q bands respectively.

4.4 Air- and space-borne instruments

The 3.5-m space-borne telescope *FIRST* (Pilbratt 1997) will carry the HIFI far-infrared/submillimetre-wave spectrometer (Whyborn 1997) and the SPIRE bolometer array camera (Griffin et al. 1998). Both of these instruments operate at frequencies for which fine-structure lines are expected to dominate the counts of line-emitting galaxies, and so the number of detectable galaxies is necessarily uncertain.

The spectral coverage of HIFI extends from 500 to 1100 GHz. The instrument will have a 4-GHz bandwidth, a 0.4-arcmin^2 field of view and a 5σ sensitivity of about $5 \times 10^{-19}\,\mathrm{W\,m^{-2}}$ in a 1-hr integration at 650 GHz. The SPIRE Fourier Transform Spectrograph (SPIRE-FTS) will provide a spectroscopic view of a 2-arcmin-square field at all frequencies between 460 GHz and 1.5 THz simultaneously. The 5σ detection threshold of a line in a 1-hr integration is expected to be about $1.5 \times 10^{-16}\,\mathrm{W\,m^{-2}}$. The slope of the counts shown in Figs 1(d) and 3(b), which are based on the estimated, and very uncertain, counts of [CII] lines, indicate that the most efficient survey depth is greater than $10^{-18}\,\mathrm{W\,m^{-2}}$ for HIFI and about $5 \times 10^{-18}\,\mathrm{W\,m^{-2}}$ for SPIRE-FTS. At a depth of $5 \times 10^{-18}\,\mathrm{W\,m^{-2}}$, the optimal detection rates using HIFI and SPIRE-FTS are expected to be about 6×10^{-3} and $7 \times 10^{-5}\,\mathrm{hr^{-1}}$ respectively, and so the detection rate of line-emitting galaxies using FIRST is expected to be quite low.

The currently quoted sensitivities of *FIRST*-HIFI are about seven times better than those of the heterodyne instruments attached to the 2.5-m SOFIA airborne telescope (Becklin 1997; Davidson 2000). Thus, when the larger field of view of SOFIA is taken into account, a line-emitting galaxy could be detected using SOFIA about every 4500 hr. Hence, SOFIA could not carry out a successful blank-field line emission survey. Note, however, that the instruments aboard SOFIA will be upgraded throughout its 20-year lifetime, and so the development of multi-element detectors and innovative wide-band spectrographs may change this situation.

The proposed space-borne far-infrared interferometer *SPECS* (Mather et al. 1998) has very great potential for resolving and obtaining very high signal-to-noise spectra of high-redshift galaxies. Although predictions of the detectability of fine-structure lines at frequencies greater than 600 GHz are very uncertain, with a field of view of about $0.25\,\mathrm{deg^{-2}}$ at 650 GHz and a 5σ sensitivity of about $10^{-18}\,\mathrm{W\,m^{-2}}$ in a 24-hr integration, about 5 [CII] galaxies could be detected per day using *SPECS* in a 8-GHz-wide band (Fig. 1d). Hence, although *SPECS* is predominantly an instrument to study known galaxies in great detail, its sensitivity is sufficient to carry out successful blank-field line surveys.

4.5 Summary of prospects for line surveys

The most promising instruments for future surveys of CO and fine-structure lines from high-redshift galaxies are the ALMA interferometer array in the 140- and 230-GHz bands, which should be able to detect about 15 galaxies an hour in a survey to a line flux density of $10^{-20}\,\mathrm{W\,m^{-2}}$ in a 16-GHz-wide band. Other instruments for which detection rates are expected to exceed one source per hundred hours are the future *SPECS* space-borne interferometer, which is likely to detect of order of five fine structure line-emitting galaxies per day, and a ground-based, wide-band, background-limited millimetre-wave grating spectrograph, which should be able to detect a line-emitting galaxy every 20 hr, the same rate as the upgraded K- and Q-band VLA.

5 CONCLUSIONS

We draw the following conclusions

(i) We have predicted the surface densities of high-redshift galaxies that emit molecular rotation and atomic fine-structure line radiation that is redshifted into the millimetre/submillimetre waveband. The results depend on both the excitation conditions in the ISM of the galaxies and the evolution of the properties of distant gas-rich galaxies. We incorporate the latest results of CO-line observations and the redshift distribution of galaxies discovered in submillimetre-wave continuum surveys to provide a sound observational basis for these predictions.

(ii) The predicted counts of CO line-emitting galaxies are probably accurate to within a factor of about 5 for lines with $J \lesssim 7$. The uncertainties are inevitable, and caused by the lack of knowledge of both the cosmological model and the excitation state of the emitting gas in the ISM of high-redshift galaxies.

(iii) The predictions of the counts of atomic fine-structure lines in high-redshift ultraluminous galaxies are more weakly constrained by observations, and we present likely order-of-magnitude estimates of the counts in six such lines.

(iv) The most efficient frequency for a survey that aims to detect CO emission is probably in the range 200–400 GHz, which includes the 230- and 350-GHz atmospheric windows. The optimal frequencies for a fine-structure line survey are probably in the range 400–800 GHz, which includes the 670- and 850-GHz atmospheric windows.

(v) There are excellent prospects for using a range of millimetre- and submillimetre-wave instruments that are currently under development to conduct blank-field surveys for the redshifted emission lines from the ISM in high-redshift galaxies. ALMA will probably prove the most capable facility for blank-field surveys, and should detect up to about 15 line-emitting galaxies per hour. The most efficient survey is likely to be made in the 140- and 230-GHz bands to a an integrated line flux density of a few $10^{-20}\,\mathrm{W\,m^{-2}}$. The required sensitivities could also be achieved by future wide-band spectrometers on single-antenna telescopes. Low-J CO transitions will be detectable using the upgraded VLA at longer millimetre and centimetre wavelengths.

(vi) A wide range of millimetre/submillimetre-wave lines should be detected in the spectra of galaxies selected in other wavebands, and in blank-field dust continuum surveys. Redshifts for millimetre/submillimetre-selected galaxies could be determined directly in these wavebands if a wide bandwidth of order $100/(1+z)$ GHz was available, with a centre frequency of about 200 GHz.

ACKNOWLEDGEMENTS

The results in this paper are based on the properties of the SCUBA lens survey galaxies detected at the Owens Valley Millimeter Array in collaboration with Aaron Evans and Min Yun. The core of the SCUBA lens survey was carried out by Ian Smail, Rob Ivison, AWB and Jean-Paul Kneib. We thank the referee Paul van der Werf for his careful reading of the manuscript and valuable comments, and also Jackie Davidson, Kate Isaak, Rob Ivison, Richard Hills, Brett Kornfeld, Malcolm Longair, Phil Lubin, Kate Quirk, John Richer and Gordon Stacey for helpful conversations and comments. AWB – the Raymond & Beverly Sackler Foundation Research Fellow at the IoA, Cambridge – gratefully acknowledges generous support from the Raymond & Beverly Sackler Foundation as part of the Deep Sky Initiative programme at the IoA. AWB thanks the Caltech AY visitors program for support while this work was conducted.

REFERENCES

Barger A. J., Cowie L. L., Sanders D. B., Fulton E., Taniguchi Y., Sato Y., Kawara K., Okuda H., 1998, Nat, 394, 248
Barger A. J., Cowie L. L., Sanders D. B., 1999a, ApJ, 518, L5
Barger A. J., Cowie L. L., Smail I., Ivison R. J., Blain A. W., Kneib J.-P., 1999b, AJ, 117, 2656
Barvainis R., Tacconi L., Antonucci R., Alloin D., Coleman P., 1994, Nat, 371, 586
Barvainis R., Maloney P., Antonucci R., Alloin D., 1997, ApJ, 484, 695
Becklin E. E., in Wilson A. ed., The Far-infrared and Submillimetre Universe. ESA SP-401, ESA publications, Noordwijk, p. 201
Blain A. W., 1996, in Shaver P. ed., Science with Large Millimetre Arrays. Springer, Berlin, p. 70
Blain A. W., 2000, in Wootten A. ed., Science with the Atacama Large Millimeter Array. Astron. Soc. Pac., San Francisco, in press (astro-ph/9911449)
Blain A. W., Longair M. S., 1993, MNRAS, 264, 509
Blain A. W., Jameson A., Smail I., Longair M. S., Kneib J.-P., Ivison R. J., 1999a, MNRAS, 309, 715
Blain A. W., Kneib J.-P., Ivison R. J., Smail I., 1999b, ApJ, 512, L87
Blain A. W., Smail I., Ivison R. J., Kneib J.-P., 1999c, MNRAS, 302, 632
Blain A. W., Ivison R. J., Kneib J.-P., Smail I., 2000, in Bunker A. J., van Breughel W. J. M. eds, The Hy-redshift universe. Astron. Soc. Pac., San Francisco, in press (astro-ph/9908024)
Bradford C. M., Stacey G. J., Swain M. R., Davidson J. A., Savage M., Jackson J. M., Bolatto A. D., 1999, http://astrosun.tn.cornell.edu/research/projects/spifi.html
Brown R. L., 1996, in Bremer M. N., van der Werf P., Röttgering H. J. A., Carilli C. R. eds, Cold Gas at High Redshift. Kluwer, Dordrecht, p. 411
Combes F., Maoli R., Omont A., 1999, A&A, 345, 369
Davidson J. A., 2000, in Lutz D., Tacconi L. eds, ULIRG 98, proceedings of Ringberg meeting September 1998. Ap&SS, in press
de Jong T., Dalgarno A., Chu S.-I., 1975, ApJ, 199, 69
Devereux N., Taniguchi Y., Sanders D. B., Nakai N., Young J. S., 1994, AJ, 107, 2006
Downes D., 1996, in Shaver P. ed., Science with Large Millimetre Arrays, Springer, Berlin, p. 16
Downes D., Solomon P., 1998, ApJ, 507, 615
Downes D., Neri R., Wiklind T., Wilner D. J., Shaver P., 1999, ApJ, 513, L1
Eales S. A., Lilly S. J., Gear W. K., Dunne L., Bond J. R., Hammer F., Le Fèvre O., Crampton D., 1999, ApJ, 515, 518
Eisenhardt P. R., Armus L., Hogg D. W., Soifer B. T., Neugebauer G., Werner M. W., 1996, ApJ, 461, 72
Erickson E. F., Colgan S. W. J., Simpson J. P., Rubin R. H., Morris M., Haas M. R., 1991, ApJ, 370, L69
Fixsen D. J., Dwek E., Mather J. C., Bennett C. L., Shafer R. A., 1998, ApJ, 508, 123
Frayer D. T., Brown R. L., 1997, ApJS, 113, 221
Frayer D. T., Ivison R. J., Scoville N. Z., Yun M. S., Evans A. S., Smail I., Blain A. W., Kneib J.-P., 1998, ApJ, 506, L7
Frayer D. T. et al., 1999, ApJ, 514, L13
Genzel R., Stacey G. J., Harris A. I., Townes C. H., Geis N., Graf U. U., Poglitsch A., Stutzki J., 1990, ApJ, 356, 160
Gerin M., Phillips T. G., 1998, ApJ, 509, L17
Griffin M. W., 1997, in Wilson A. ed., The Far-Infrared and Submillimetre Universe. ESA publications, Noordwijk, p. 31
Griffin M. W. et al., 1998, SPIRE proposal document, http:/www.ssd.rl.ac.uk/spire
Guiderdoni B., Hivon E., Bouchet F. R., Maffei B., 1998, MNRAS, 295, 877
Hauser M. G. et al., 1998, ApJ, 508, 25
Holland W. S. et al., 1999, MNRAS, 303, 659
Hughes D. H. et al., 1998, Nat, 394, 241
Isaak K., McMahon R., Hills R., Withington S., 1994, MNRAS,

268, L28
Isaak K., Harris A. I., Zmuidzinas J., 1999, in Carilli C. L., Radford S. J. E., Menten K., Langston G., Highly Redshifted Radio Lines. Astron. Soc. Pac., vol. 156. San Francisco, p. 86
Ishiguro M., Kawabe R., Nakai N., Morita K.-I., Okumura S. K., Ohashi N., 1994, in Ishiguro M., Welch W. J. eds, Astronomy with millimeter and submillimeter interferometry, Astron. Soc. Pac., vol. 59. San Francisco, p. 405
Ivison R. J., Harrison A. P., 1996, A&A, 309, 461
Ivison R. J., Harrison A. P., Coulson I. M., 1998a, A&A, 330, 443
Ivison R. J., Papadopoulos P., Seaquist E. R., Eales S. A., 1996, MNRAS, 278, 669
Ivison R. J., Smail I., Le Borgne J.-F., Blain A. W., Kneib J.-P., Bézecourt J., Kerr T. H., Davies J. K., 1998b, MNRAS, 298, 583
Ivison R. J., Smail I., Barger A. J., Kneib J.-P., Blain A. W., Owen F. N., Kerr T. H., Cowie L. L., 2000, MNRAS, in press (astro-ph/9911069)
Kawara K. et al., 1998, A&A, 336, L9
Kneib J.-P., Alloin D., Mellier Y., Guilloteau S., Barvainis R., Antonucci R., 1998, A&A, 329, 827
Lewis G. F., Chapman S. C., Ibata R. A., Irwin M. J., Totten E. J., 1998b, ApJ, 1998b, 505, L1
Lilly S. J., Eales S. A., Gear W. K. P., Hammer F., Le Fevre O., Crampton D., Bond J. R., Dunne L., 1999, ApJ, 518, 641
Loeb A., 1993, ApJ, 404, L37
Luhman M. et al., 1998, ApJ, 504, L11
Lutz D., Spoon H. H. W., Rigopoulou D., Moorwood A. F. H., Genzel R., 1998, ApJ, 505, L103
Malhotra S. et al. 1997, ApJ, 491, L27
Mather J. C. et al., 1998, preprint (astro-ph/9812454)
Mauersberger R., Henkel C., Walsh W., Schulz A., 1999, A&A, 343, 939
Nikola T., Genzel R., Herrmann F., Madden S. C., Poglitsch A., Geis N., Townes C. H., Stacey G. J., 1998, ApJ, 504, 749
Ohta K., Yamada T., Nakanishi K., Kohno K., Akiyama M., Kawabe R., 1996, Nat, 382, 426
Ohta K, Nakanishi K, Akiyama M, Yamada T, Kohno K, Kawabe R, Kuno N, Nakai N, 1998, PASJ, 50, 303
Omont A., Petitjean P., Guilloteau S., McMahon R. G., Solomon P. M., Pécontal E., 1996, Nat, 382, 428
Pierini D., Leech K. J., Tuffs R. J., Völk H. J., 1999, MNRAS, 303, L29
Pilbratt G., 1997, in Wilson A. ed., The Far-Infrared and Submillimetre Universe. ESA publications, Noordwijk, p. 7
Puget J.-L. et al., 1999, A&A, 345, 29
Sanders D. B., Scoville N. Z., Young J. S., Soifer B. T., Schloerb F. P., Rice W. L., Danielson G. E., 1986, ApJ, 305, L45
Saunders W., Rowan-Robinson M., Lawrence A., Efstathiou G., Kaiser N., Ellis R. S., Frenk C. S., 1990, MNRAS, 242, 318
Schlegel D. J., Finkbeiner D. P., Davis M., 1998, ApJ, 500, 525
Silk J., Spaans M., 1997, ApJ, 488, L79
Smail I., Ivison R. J., Blain A. W., 1997, ApJ, 490, L5
Smail I., Ivison R. J., Blain A. W., Kneib J.-P., 1998, ApJ, 507, L21
Smail I., Ivison R. J., Blain A. W., Kneib J.-P., 1999, in Holt S. S., Smith E. P. eds., After the dark ages: when galaxies were young. AIP Woodbury NY, p. 312 (astro-ph/9810281)
Smail I., Ivison R. J., Owen F. N., Blain A. W., Kneib J.-P., 2000, ApJ, in press (astro-ph/9907083)
Soifer B., Neugebauer G., 1991, AJ, 101, 354
Solomon P. M., Downes D., Radford S. J. E., 1992, ApJ, 398, L29
Stacey G. J., Geis N., Genzel R., Lugten J. B., Poglitsch A., Sternberg A., Townes C. H., 1991, ApJ, 373, 423
Stacey G. J., Bradford C. M., Swain M. R., Jackson J. M., Bolatto A. D., Davidson J. A., Savage M., 1996, in Pilbratt G., Rolfe E. eds, Submillimetre and Far-Infrared Space Instrumentation, ESA SP-388, ESA publications, Noordwijk, p. 139
Stark A. A., 1997, ApJ, 481, 587
van der Werf P. P., 1999, in Carilli C. L., Radford S. J. E., Menten K., Langston G., Highly Redshifted Radio Lines. Astron. Soc. Pac., vol. 156. San Francisco, p. 91
van der Werf P. P., Israel F. P., 1997, in Shaver P. A. ed., Science with Large Millimetre Arrays. Springer, Berlin, p. 51
Whyborn N. D., 1997, in Wilson A. ed., The Far-Infrared and Submillimetre Universe. ESA publications, Noordwijk, p. 19
Wild W., Harris A. I., Eckart A., Genzel R., Graf U. U., Jackson J. M., Russell A. P. G., Stutzki J., 1992, A&A, 265, 447
Wootten A., 2000, Science with the Atacama Large Millimeter Array. Astron. Soc. Pac., San Francisco, in press
Wright E. L. et al., 1991, ApJ, 381, 200